2006 International Joint Conference on Neural Networks
Sheraton Vancouver Wall Centre Hotel, Vancouver, BC, Canada
July 16-21, 2006

Sensorless ANN-Based Speed Estimation of Synchronous Generators: Improved Performance through Physically Motivated Pre-filters

Innocent Kamwa, *Fellow, IEEE*, Bogdan Baraboi, *Non Member*, and René Wamkeue, *Member, IEEE*

Abstract—**This paper deals with an improved approach for estimation of generator rotor speed in power systems. We propose a hybrid speed estimator, which combines classical approach, based on a mathematical model of the electrical machine, with AI-based approach, implemented by an artificial neural network (ANN). The classical estimation model processes the machine stator voltages and currents and provides intermediary information on the generator speed. The ANN component acts as a function approximator, mapping the intermediary speed components to a more reliable estimation of the generator speed. Multi-layer feedforward ANNs are used for this purpose. Data for training the ANN are obtained through off-line simulations of a generator operating in a two-machine model. After ANN design and training, the performance of the hybrid estimator is tested with simulated on-line measurements in a wide range of operating conditions. Results obtained with the hybrid estimator are compared against those provided by a classical mathematical model-based estimator and an AI-based estimator.**

Index Terms **-- Artificial neural networks, dynamic security assessment, rotor speed estimation, synchronous machine, transient stability.**

I. Introduction

THE development of power systems and the increasing demand for energy quality, and lower costs continuously stimulate the investigation of new control techniques to enhance power system stability. This is more so since economic considerations push the operation of power systems closer to their stability limits.

Accurate information about synchronous generators speed is necessary to realize high-performance dynamic security assessment and control of power system. In recent years, speed-sensorless control methods of electrical machines, using the estimated speed instead of the measured speed, are attracting increased interest. This solution seems to be an efficient alternative to the traditional speed sensors, resulting in increased robustness and reliability, increased simplicity, reduced costs, and decreased maintenance requirements [1],[2]. Vas [2] classifies the speed estimators used in speed sensorless drives as "classical" and "artificial intelligence-based" (AI) types. In general, the classical approaches utilize a mathematical model of the electrical machine and also require the knowledge of some machine parameters. The most popular types of model-based speed estimators are the model reference adaptive system (MRAS) and observer based estimators (Kalman filter, Luenberger observer) [2], [3].

Unlike the classical models, the AI-based speed estimators can describe the non-linear behavior of the machine without requiring a mathematical model or any machine parameters. The artificial neural networks and fuzzy-neural networks are trainable dynamical systems capable to estimate input-output functions by learning from experience with numerical and, sometimes, linguistic sample data. They are model-free estimators [4]. Moreover, they have the advantages of fast parallel computation and fault tolerance characteristics. The intense research in this field demonstrated that the AI-based speed estimators can lead to improved performance, being robust to parameter variation, adaptive and easy to extend, and not computationally demanding [2], [3], [5]-[10].

However, practical applications of the AI-based implementations in speed estimators are still scarce, underpinning the need for more research in this area. In contrast to the classical "knowledge-based models", the traditional view of artificial neural networks (ANN) is that of "black-box models", i.e. models that are obtained only from data, and that not include any analysis of the non-linear dynamical system [11]. Moreover, the performance of the ANN estimator greatly depends on the training set, making the selection of data crucial.

In this paper, we propose a speed estimator which intends to combine the best characteristics of the two approaches: the legibility of knowledge-based models and the flexibility of training from experimental data. A hybrid system was generated by associating an existing mathematical-based model with an artificial neural network. It was designed to estimate the rotor speed of a synchronous generator. First, the structure of the hybrid speed estimator is presented. Then, the operation of the classical model and the development methodology of the ANN-based component are described. Finally, an analysis of the estimator performance is carried out. Simulation results, obtained using a wide range of operating conditions, are shown to illustrate the validity of the proposed solution.

I. Kamwa, is with Hydro-Québec, IREQ 1800 boul. Lionel-Boulet, Varennes, Qc, Canada J3X 1S1 (e-mail: kamwa.innocent@ireq.ca) .
B. Baraboi was a graduate student in Electrical Engineering a Laval University, Qc, Canada. At present he is with Ariane Controls (e-mail: bbaraboi@arianecontrols.com).
R. Wamkueue is with Universite du Quebec en Abittibi-Temiscamingue, (e-mail: rene.wamkeue@uqat.ca).

II. STRUCTURE OF THE HYBRID SPEED ESTIMATOR

Figure 1 shows the structure of the proposed hybrid speed estimator. It consists of two components: a classical estimation model (named pre-processor) and an intelligent system, implemented by an ANN.

The pre-processor performs an initial estimation of the synchronous machine (SM) speed, from the instantaneous values of stator voltages and currents (V_{abc}, I_{abc}). Using a mathematical model of the machine, the pre-processor provides two intermediary values of the speed (ω_{LF}, ω_{HF}). These signals represent the input of the intelligent system (ANN), which acts as a function approximator. The final estimated speed (ω_e) is obtained at the output of the ANN.

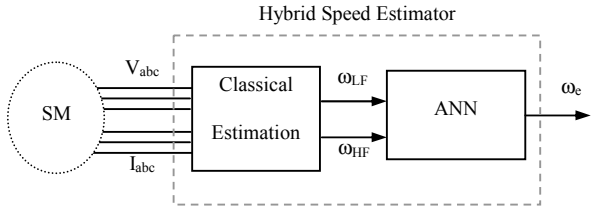

Fig. 1. Structure of hybrid speed estimator

Design considerations for the two components of the hybrid system are presented in the following sections. Estimator development and performance analysis were carried out using Matlab/Simulink computing environment, together with associated toolboxes.

III. CLASSICAL MODEL DESCRIPTION

The pre-processor represents the "classical" component of our hybrid estimator. It has the role to pre-process the measured signals (stator voltages and currents) and to provide intermediary information on the SM speed. The pre-processor was designed as a mathematical model-based estimator, based on the generator electro-mechanical equations.

Two components of the rotor speed are obtained at the output of the pre-processor: a low-frequency component (ω_{LF}), calculated from the voltage equation, and a high-frequency component (ω_{HF}), deduced from the electrical power.

First, the positive-sequence components of voltage and current (V_p, I_p) are calculated. By applying the Clarke transformation for measured three-phase quantities (V_a, V_b, V_c; I_a, I_b, I_c), we obtain:

$$\begin{bmatrix} V_d \\ V_q \end{bmatrix} = \frac{1}{3} \begin{bmatrix} 1 & -\frac{1}{2} & -\frac{1}{2} \\ 0 & \frac{\sqrt{3}}{2} & -\frac{\sqrt{3}}{2} \end{bmatrix} \cdot \begin{bmatrix} V_a \\ V_b \\ V_c \end{bmatrix} \quad (1)$$

The transformation is the same for the case of the three-phase current (I_d, I_q).

The stator space vectors are defined as complex quantities, having V_d and V_q (or I_d and I_q) as rectangular coordinates:

$$v_p = V_d + jV_q; \qquad i_p = I_d + jI_q \quad (2)$$

The positive-sequence components (V_p, I_p) are then obtained by applying the DFT (Discrete Fourier Transformation) on the voltage and current space vectors.

The synchronous machine is represented by a simplified model, generally used in transient stability studies, called the classical generator model [12]:

$$E' = E'\angle\delta = V_p + jX_q I_p \quad (3)$$

where E' is the constant internal voltage, V_p is the generator terminal voltage, X_q is the q-axis reactance, and I_p is the generator terminal current.

Having calculated the positive-sequence components (V_p, I_p), and knowing the value of X_q, the rotor speed can be approximated as:

$$\omega(t) = \omega_{syn} + \frac{d\delta(t)}{dt} \quad (4)$$

where ω_{syn} is the synchronous speed [12].

A low pass filter is then applied to eliminate the noise, generating the low-frequency speed component (ω_{LF}). The high-frequency speed component, ω_{HF}, is obtained by integrating the electrical power from the equation that determines rotor dynamics (in per-unit system):

$$2H\frac{d\omega}{dt} = P_m - P_e \quad (5)$$

where H is the inertia constant, P_m is the mechanical power supplied by the prime mover minus mechanical losses, P_e is the electrical power output of the generator plus electrical losses.

The P_m factor is considered constant in equation 5. This approximation is valid since it is known that during a transient event the mechanical power changes are negligible. So, we can see that the ω_{HF} speed component is 1/2H times the integral of the electrical power.

A low pass filter and a high pass filter were designed for the two speed components, in order to minimize the delays and to reduce the differences between real speed and estimated speed.

A reliable speed estimator was developed based on this approach. It is able to provide a good estimation of SM speed during the steady-state, but also during the transient. The low-frequency speed component calculated from stator voltage characterizes the slow phenomena. The high-frequency speed component deduced from the electric power led to the improvement of the estimation precision, in particular in the presence of fast phenomena.

However, this classical estimator is based on a mathematical modeling of the synchronous machine that implies several assumptions: machine excitation is constant, machine losses, saturation, and saliency are neglected, etc. All these assumptions impose some limit to the system

performance. In addition, a priori knowledge of some machine parameters is required by the simple equations (3, 5). More detailed generator model aiming to improved accuracy would require proper machine parameter identification.

By associating an AI-based technique to the classical estimator, we expect to improve its stability and robustness and to obtain a more effective speed estimator, which does not rely on knowledge of any machine parameters.

IV. DEVELOPMENT OF ANN COMPONENT

The role of the AI-based system is to map the two speed components (ω_{LF}, ω_{HF}) provided by the pre-processor to a reliable estimation of the generator rotor speed. For this purpose, we use multi-layer feedforward ANN, which views estimation as a "curve-fitting" problem.

The multi-layer feedforward networks are indisputably the most used ANN in applications [13, 14, 15]. It has been shown that they are universal approximators [16], i.e. the multi-layer feedforward networks are capable to approximate any measurable function in a very precise and satisfactory manner, if a sufficient number of hidden neurons are used. However, there are a number of practical concerns, as the selection of training data, the choosing of network architecture, the time complexity of learning, the ability of network to generalize. The main steps followed in the ANN development are presented in this section.

A. Data base generation

The selection of the appropriate data for the ANN training and testing is very important factor for its performance. The training data must represent all possible transient and steady-state characteristics of the synchronous machine under consideration. Moreover, a reliable speed estimator should have an extremely good generalization, being able to provide good estimates in any condition and independent of power system behavior. However, it is difficult to include all particular characteristics of the system in the training set. The most significant patterns must be carefully selected in order to obtain the best estimation capabilities.

Figure 2 depicts the power system model used to generate the ANN data base. The system was implemented using the SimPowerSystems tool in the Simulink environment [17]. This simplified model is very helpful in the study of transient stability of multi-machine systems. It enables us to simulate the dynamic behavior of a synchronous generator to different disturbances.

A 1000 MW hydraulic generation plant (machine M1) is connected to a load center through a long 500 kV, 700 km transmission line. The load center is modeled by a 5000 MW resistive load. The load is fed by the remote 1000 MW plant and by a local generation of 5000 MW (machine M2). The system has been initialized so that the line carries 950 MW, which is close to its Surge Impedance Loading (SIL = 977 MW). The two machines are equipped with identical 'Turbine and Regulator' subsystems, which include the Hydraulic Turbine and Governor (HTG), the Excitation system and the Power System Stabilizer (PSS). Appendix I lists the machine model parameters used in simulation for data base generation.

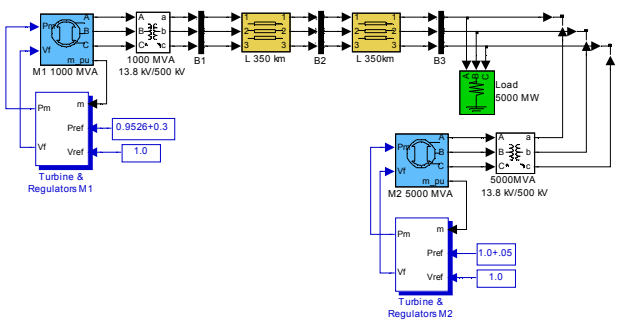

Fig. 2. Simulink diagram of two-machine power system used for data base generation

Only the behavior of the synchronous machine M1 was considered in the development of the data base. Instantaneous values (in p.u.) of stator voltages and currents (V_{abc1}, I_{abc1}) and of the rotor speed (ω_{M1}) are recorded at each simulation. Then, the intermediate speed components ω_{LF}, ω_{HF} are obtained using the pre-processor system.

An experimental design procedure involving extensive simulation studies was applied in order to obtain efficient training data and to avoid redundant information. At each design step, new scenarios were simulated to reproduce the system behavior. To analyze the efficiency of the selected patterns, a neural network was trained with data acquired after each step.

First, small-signal stability of the power system was considered. Different small disturbances were simulated, by setting pulse changes in voltage reference (V_{ref1}) and in power reference (P_{ref1}) of generator M1. The pulses had magnitudes between 5% and 20% and durations from 6 to 24 cycles.

Then, power system behavior under large disturbances was simulated. Following a large perturbation, the system is either transiently stable, reaching a new equilibrium state, or instable, resulting in a run-away or run-down situation. The contingencies considered are different types of short-circuit applied at bus B1: single line-to-ground fault, line-to-line fault, double line-to-ground fault and balanced three-phase fault. The faults were released by self-clearance, having durations chosen between 1 and 20 cycles. Stable and unstable cases were included in the data base.

Afterward, to develop the robustness and the generalization capacity of the speed estimator, changes in machine parameters were considered in data base selection. A methodical analysis was performed to study the influence of various parameters on the generator behavior, under different contingencies. As a result of this analysis, all the simulations, including small and large disturbances, were performed for three different values of machine inertia

constant: H = 2 pu-s, H = 3.7 pu-s and H = 6 pu-s.

Some additional simulations were carried out for values of H different from 2, 3.7 and 6 (but also located in range [2, 6]). This data was used only for ANN testing.

A sampling interval of 5 ms was used in all simulations carried out in data base development. The duration of each simulation was selected to give a balance of transient and steady-state information. The final data base contains 219817 samples, acquired in 327 simulations. It is composed of two sets:

- A training data set, including ~72% of the available data (236 simulations, i.e. 158849 samples), developed to design and train the ANN.
- A testing data set, including ~28% of the acquired data (91 simulations, i.e. 60968 samples), built to test the ANN.

Tables I and II summarize the distribution of simulations carried out in data base generation for training and testing set, respectively.

TABLE I
DISTRIBUTION OF SIMULATIONS IN GENERATION OF TRAINING DATA SET

Inertia cst.	Small signal		Large disturbances (faults at bus B1)							
	ΔV_{refl}	ΔP_{refl}	line-to-gnd faults		line-to-line faults		double line-to-gnd faults		three-phase faults	
			stable	instable	stable	instable	stable	instable	stable	instable
H=2	25	8	9	4	4	5	5	5	4	7
H=3.7	25	8	10	3	10	4	7	4	5	6
H=6	25	8	13	1	9	3	6	4	4	5

TABLE II
DISTRIBUTION OF SIMULATIONS IN GENERATION OF TESTING DATA SET

Inertia cst.	Small signal		Large disturbances (faults at bus B1)							
	ΔV_{refl}	ΔP_{refl}	line-to-gnd faults		line-to-line faults		double line-to-gnd faults		three-phase faults	
			stable	instable	stable	instable	stable	instable	stable	instable
H=2	6	2	3	1	1	1	2	1	1	1
H=3.7	6	2	3	1	4	2	3	3	2	3
H=6	6	2	5	0	3	1	2	1	1	1
H≠2, 3.7, 6	3	2	3	1	2	2	2	2	2	2

After the data base was created, the inputs (ω_{LF}, ω_{HF}) and targets (ω) were normalized to lie in the interval [0, 1].

B. ANN design

The *Neural Network Toolbox* from Matlab was used to design, train and test the feedforward ANN.

The ANN design is a complex iterative process, based on trial and error method. Its purpose is to determine the optimal architecture of the neural network (e.g. number of inputs, number of hidden layers, and number of hidden neurons) and to choose the optimal training parameters (e.g. performance goal, learning rate, numbers of epochs to train, minimum performance gradient, etc).

Only the training data base has been used in the design process. In order to get the best network performance, a division of the available data into two subsets was performed. The first subset is the training set, which is used for computing the gradient and updating the network weights and biases. Several different backpropagation training algorithms were experienced, like Levenberg-Marquardt, scaled conjugate gradient, and BFGS quasi-Newton. The second subset is the validation set, which is used to prove the network generalization capability. The choice of the validation subset is very important. The validation data should be representative of all points in the training subset. The error on the validation set is monitored during the training process. When the network begins to overfit the data, the error on the validation set will typically begin to rise. When the validation error increases for a specified number of iterations, the training is stopped, and the weights and biases at the minimum of the validation error are returned [18].

Additionally, multiple runs of the training/validation experiment were performed in order to avoid random influences (e.g. weight initialization, specific division of data, and sequence of training data) [19]. The computation of multiple runs also gives a better estimate of the network performance. This technique consists in repeating several times the training/validation of each ANN, using various configurations of the data base. For this purpose, three different configurations of the training and validation subsets were generated. For each configuration, the training/validation process was repeated five times, the data in the two subsets being initially well shuffled.

A large number of neural networks with one and two hidden layers were experienced at this stage. Topologies with different number of inputs, and one and two hidden layers were considered. Some typical examples are presented in table III.

TABLE III
DESIGN RESULTS FOR VARIOUS ANN ARCHITECTURES

ANN inputs	ANN architecture	Training MSE		Validation MSE	
		mean	variance	mean	variance
$\omega_{LF}(k)$, $\omega_{HF}(k)$	2-5-1	9.76×10^{-6}	2.32×10^{-13}	1.06×10^{-5}	1.64×10^{-12}
H, $\omega_{LF}(k)$, $\omega_{HF}(k)$	3-7-1	9.59×10^{-6}	1.29×10^{-12}	1.01×10^{-5}	5.03×10^{-12}
$\omega_{LF}(k-1)$, $\omega_{LF}(k)$, $\omega_{HF}(k-1)$, $\omega_{HF}(k)$	4-10-1	4.24×10^{-6}	1.18×10^{-14}	4.39×10^{-6}	1.54×10^{-14}
$\omega_{LF}(k-5)$, $\omega_{LF}(k)$, $\omega_{HF}(k-5)$, $\omega_{HF}(k)$	4-10-1	5.38×10^{-6}	1.21×10^{-12}	5.67×10^{-6}	1.44×10^{-12}
$\omega_{LF}(k-1)$, $\omega_{LF}(k)$, $\omega_{HF}(k-1)$, $\omega_{HF}(k)$	4-6-4-1	5.30×10^{-6}	7.09×10^{-13}	5.51×10^{-6}	7.7×10^{-13}
H, $\omega_{LF}(k-1)$, $\omega_{LF}(k)$, $\omega_{HF}(k-1)$, $\omega_{HF}(k)$	5-7-4-1	4.17×10^{-6}	6.29×10^{-14}	4.36×10^{-6}	7.03×10^{-14}
$\omega_{LF}(k-2)$, $\omega_{LF}(k-1)$, $\omega_{LF}(k)$, $\omega_{HF}(k-2)$, $\omega_{HF}(k-1)$, $\omega_{HF}(k)$	6-14-1	3.69×10^{-6}	3.5×10^{-14}	3.86×10^{-6}	4.26×10^{-14}

As a measure of performance in the training/validation process, two statistical indexes were computed for each ANN topology:

- The mean of MSE:

$$\mu = \frac{\sum_i MSE_i}{N} \qquad (6)$$

Where, *MSE* is the mean squared error between the true and the estimated rotor speed, N = 15 is the number of runs of each experiment.

- The variance:

$$\sigma^2 = \frac{\sum_i (MSE_i - \mu)^2}{N} \qquad (7)$$

After considerable studies, a 4-10-1 ANN topology was selected. It provides a satisfactory balance between accuracy level, convergence speed, and network complexity. The ANN has 4 inputs, representing the present and past values of the intermediary speed components provided by the pre-processor: $\omega_{LF}(k\text{-}1)$, $\omega_{LF}(k)$, $\omega_{HF}(k\text{-}1)$, $\omega_{HF}(k)$. The hidden layer contains 10 neurons, and the activation function is the hyperbolic tangent sigmoid. The output layer contains a single linear neuron, which provide the actual value of the rotor speed: $\omega(k)$.

C. ANN training and testing

The entire training data set (including both training and validation subsets) was used for learning the selected ANN with now optimized parameters. ANN 4-10-1 was trained using the Levenberg-Marquardt algorithm, which provides the fastest convergence and very accurate learning. The network was trained for 200 epochs using a mean squared error index of 3.5×10^{-6} as performance goal.

Then, the network was finally tested with the remaining, never before used testing set, which contains ~28% of the acquired data base, i.e. 60968 samples. As a measure of performance, the mean relative error (MRE) between the true and estimated rotor speed was computed in the testing stage.

In order to avoid random influences on learning convergence and to obtain a better estimate of the ANN performance, multiple runs of the training/testing experiment were computed. The 232 contingencies in the training set were well shuffled before training, to enhance randomness of the data and minimize sequential bias effect. The process was repeated 15 times. After each training/testing cycle, the neural network parameters were saved, as well as the MRE over the 60968 testing patterns. When a new model provided a smaller MRE, it replaced the previous best model. Mean and variance of testing errors on the 15 runs of the experiment were calculated: μ_{MRE} = 1.64×10^{-4}, σ^2 = 1.73067×10^{-11}. The ANN retained at the end of the training/testing process is characterized by a performance index MRE = 1.6×10^{-4}.

V. PERFORMANCE ANALYSIS OF HYBRID SPEED ESTIMATOR

To analyze the performance of the hybrid estimator in online conditions, the estimator was used to provide the speed feedback signal in a simulated closed-loop PID governor system associated to a synchronous generator. The simulations were carried out using Simulink environment.

Figure 3 shows the Simulink block diagram of the hybrid estimator. The V_{abc}, I_{abc} sensor system measures the instantaneous values of the stator voltages and currents of the synchronous machine, which are the inputs of the classical pre-processor system. Data acquired in all real-time environments is noise corrupted. Contributing factors include excitation system AC to DC rectification process, quantization errors in sensors, surrounding electromagnetic interference, etc. [20]. To investigate the effect of noise on the estimator performance, uniformly distributed noise in the range [-0.1, 0.1] is added to voltage and current signals.

The classical pre-procesor model requires some parameters

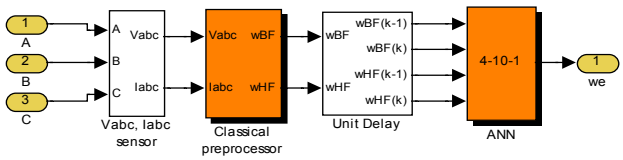

Fig. 3. Simulink block diagram of hybrid speed estimator

of synchronous machine: the inertia constant H and the quadrature axis subtransient reactance X_q''. Constant values of these parameters were used by the pre-processor in all simulations: H = 3.7 pu-s; X_q'' = 0.243 pu. The unit delay system normalizes data and generates present and past values of the two intermediary speed components, producing the appropriate ANN input signals. The 4-10-1 artificial neural network trained in Matlab was converted in a Simulink block (ANN).

Performance analysis was performed by comparing the results provided by the hybrid estimator to those obtained using a classical mathematical model and an AI-based estimator. In the classical approach, the speed is computed by simply adding the two components provided by the pre-processor system (ω_{LF}, ω_{HF}). The AI-based estimator is implemented by a simple feedforward neural network that estimates the speed directly from machine stator voltages and currents. The ANN was created using the existing data base. A similar trial and error based methodology as described in section IV was applied to design, train, and test the ANN-based estimator. A final network with 12-30-1 architecture was selected. The ANN inputs are the sampled values of the real and imaginary parts of positive sequence components of stator voltage and current, at three successive instants: *Vp_re*(*k-2*), *Vp_re*(*k-1*), *Vp_re*(*k*), *Vp_im*(*k-2*), *Vp_im*(*k-1*), *Vp_im*(*k*), *Ip_re*(*k-2*), *Ip_re*(*k-1*), *Ip_re*(*k*), *Ip_im*(*k-2*), *Ip_im*(*k-1*), *Ip_im*(*k*). The hidden layer contains 30 neurons using the tangent sigmoid activation function. The output neuron is linear and provides the present value of the speed.

Extensive simulation studies have been carried out to

investigate the performance of the speed estimators incorporated in the closed-loop governor system of a synchronous generator. Various scenarios not used in the data base generation were simulated, including different disturbances, deviation of machine parameters, different types of synchronous generators, and various power system topologies. Some typical results are presented in the following sections.

For illustration purposes, the evolution of actual and estimated rotor speed is plotted for different circumstances. The actual values of the rotor speed are those extracted directly from the synchronous machine Simulink model. The estimated speed values are obtained using the classical, the AI-based, and the hybrid estimators. For comparison, the mean relative error (*MRE*) between the actual and the estimated speed was computed for the three types of estimators.

A. Two-machine test system

The first tests have been carried out by simulating the estimators operation in the two-machine power system model used in data base generation stage. Performance of the three estimators to a small disturbance is exemplified in figure 4.

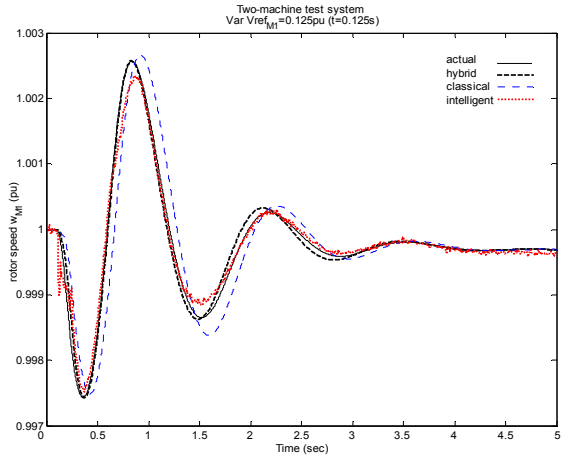

Fig. 4. Actual and estimated speed of generator M1 - small disturbance

A 12.5% magnitude-pulse was applied for 7.5 cycles to the voltage reference of M1 (V_{ref1}). Estimator robustness to machine parameter changes was also investigated in this simulation, by varying the inertia constant and the direct axis subtransient reactance of the two machines (H = 3.55 pu-s, X_d'' = 0.35 pu). The three estimators were successively used to estimate the speed of generator M1. It can be seen from figure 4 that all three systems provide a quite satisfactory estimation of the rotor speed, but better accuracy was obtained using the proposed hybrid estimator.«The errors computed for the three models prove this remark: $MRE_{hybrid} = 6.60\times10^{-5}$, $MRE_{classical} = 2.23\times10^{-4}$, $MRE_{AI\text{-}based} = 2.20\times10^{-4}$.

Figure 5 presents a stable response to a large perturbation, i.e. a double line-to-ground fault at bus B1, cleared in 5.5 cycles. Changes in inertia constant and quadrature axis subtransient reactance were also considered: H = 3.1pu-s, X_q'' = 0.29 pu. The performance of the three estimators is characterized by the following errors: $MRE_{hybrid} = 1.42\times10^{-4}$, $MRE_{classical} = 8.91\times10^{-4}$, $MRE_{AI\text{-}based} = 3.62\times10^{-4}$. The proposed hybrid system outperforms the classical and AI-based approaches. Figures 4 and 5 illustrate that the classical estimator is characterized by a phase error during speed oscillations.

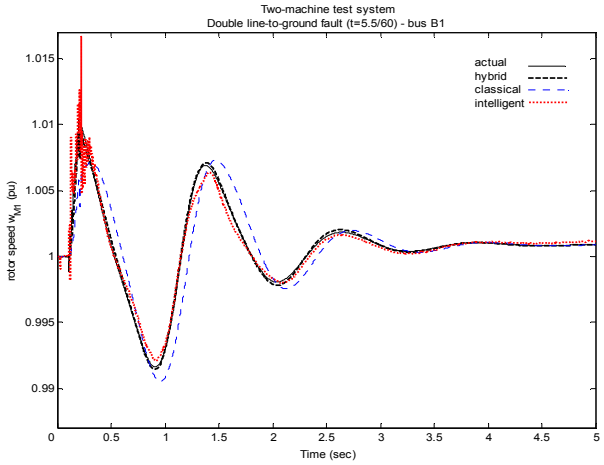

Fig. 5. Actual and estimated speed of generator M1 – large disturbance, stable case

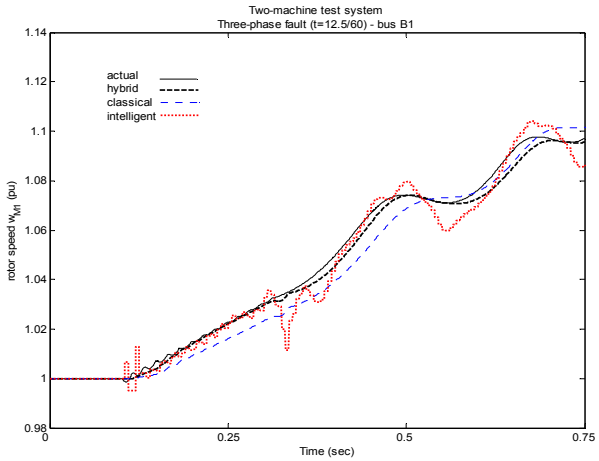

Fig. 6. Actual and estimated speed of generator M1 - large disturbance, instable case

An unstable case is illustrated in figure 6. A three-phase to ground fault was simulated at bus B1 for 12.5 cycles. New values of inertia constant and quadrature axis subtransient reactance were considered: H = 2.7pu-s, X_q'' = 0.15 pu. Again, better tracking of M1 rotor speed was obtained when using the hybrid estimator. For comparison, the estimation errors were calculated: $MRE_{hybrid} = 2\times10^{-3}$, $MRE_{classical} = 4.3\times10^{-3}$, $MRE_{AI\text{-}based} = 3.7\times10^{-3}$.

Disturbances occurring in different locations of the two-machine power system were also simulated in the test stage. Remember that only contingencies at the machine M1 side of

the transmission line (bus B1) have been considered in data base generation. Figure 7 shows the results of M1 speed estimation in the case of an 8-cycle, single line-to-ground fault simulated at bus B3. The performance of the three estimators is characterized by the following errors: $MRE_{hybrid} = 1.65\times10^{-4}$, $MRE_{classical} = 2.36\times10^{-4}$, $MRE_{AI\text{-}based} = 4.3\times10^{-3}$. These show a degraded performance of the AI-based estimator in comparison with that of the hybrid and the classical estimators.

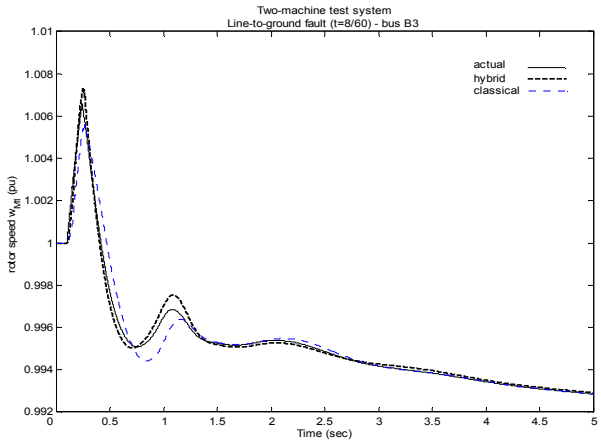

Fig. 7. Actual and estimated speed of generator M1 - disturbance applied at bus B3

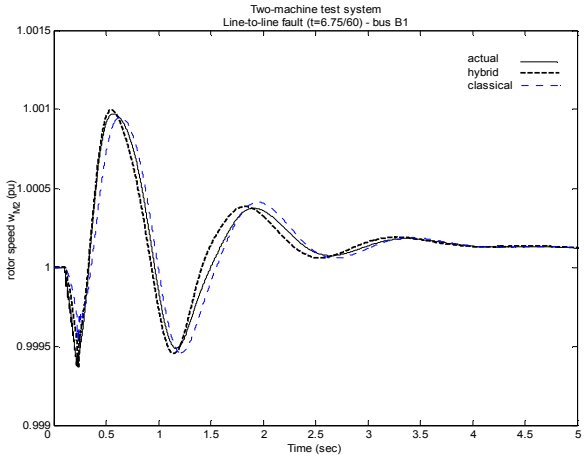

Fig. 8. Actual and estimated speed of generator M2 - disturbance applied at bus B1

The three estimators were also tested to provide the speed of the M2 generator in the two-machine power system. It should be noted that only the behavior of the M1 generator was considered in the development of the data base. Again, the AI-based estimator cannot provide correct speed estimation. In contrast, the classical and the hybrid estimators continue to give a satisfactory performance. As an example, results obtained with these two estimators for M2 generator speed in the case of a 6.75-cycle line-to-line fault simulated at bus B1 are shown in figure 8. Different inertia constants of the two generators were also considered in this simulation: $H_{M1} = 4.05$ pu-s, $H_{M2} = 3$ pu-s. The errors indicate that both classical and hybrid estimators predict accurately the speed of M2 generator, but the AI-based estimator fails: $MRE_{hybrid} = 3.5\times10^{-5}$, $MRE_{classical} = 4.36\times10^{-5}$, $MRE_{AI\text{-}based} = 1.25\times10^{-2}$.

B. Four-machine test system

Subsequently, the performance of the three estimators was analyzed by simulating their closed-loop response in other Simulink models, representing different topologies of power systems. As expected, the AI-based estimator did not give satisfactory results, since the ANN has only been trained using the two-machine power system model. On the other hand, it should be noted that the hybrid and the classical estimators are able to generalize, and can provide quite accurate estimates of the speed for different types of synchronous generators in various power system topologies.

For illustration purposes, the performance of the classical and hybrid estimators in a four-machine two-area test system is presented. The power system consists of two fully symmetrical areas linked together by two 230 kV lines of 220 km length (figure 9). This system was specifically designed in [21], [22] to study low frequency electromechanical oscillations in large interconnected power systems. Each area is equipped with two identical round rotor generators rated 20 kV/900 MVA. The synchronous machines have identical parameters, except for inertias which are $H = 4.5$ pu-s in area 1 and $H = 6.175$ pu-s in area 2 (see appendix II). Thermal plants having identical speed regulators are further assumed at all locations.

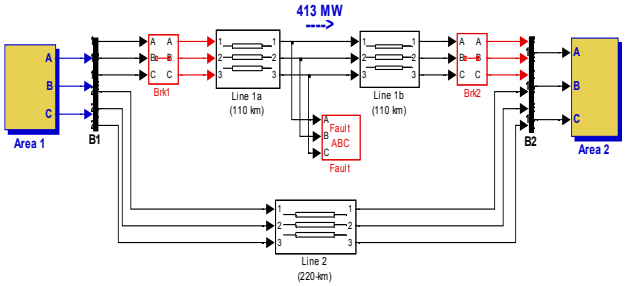

Fig. 9. Simulink diagram of four-machine two-area power system used for estimator performance analysis

The three estimators were succesively used to provide the speed of the four machines. A variety of tests were performed, including small and large perturbations, and the use of three types of power system stabilizers (MB-PSS, Delta w PSS, and Delta Pa PSS).

Figures 10 to 13 illustrates the results obtained using the classical and the hybrid estimators in the case of a three-phase fault cleared in 8 cycles by opening the brakers Brk1 and Brk2. MB-PSS with simplified settings (IEEE Std 421.5) was used in this simulation to maintain the system stability. It can be seen that the two models provide quite satisfactory estimation of the speed for all generators: $MRE_{hybrid} = 1.65\times10^{-4}$, $MRE_{classical} = 1.3\times10^{-4}$ (machine M1),

MRE_{hybrid}=1.96×10^{-4}, $MRE_{classical}$ = 1.62×10^{-4} (machine M2), MRE_{hybrid} = 1.96×10^{-4}, $MRE_{classical}$ = 2.09×10^{-4} (machine M3), MRE_{hybrid} = 1.86×10^{-4}, $MRE_{classical}$ = 2.54×10^{-4} (machine M4). It should be noted the excellent performance of the hybrid estimator in conditions very different from those used in the development of the ANN.

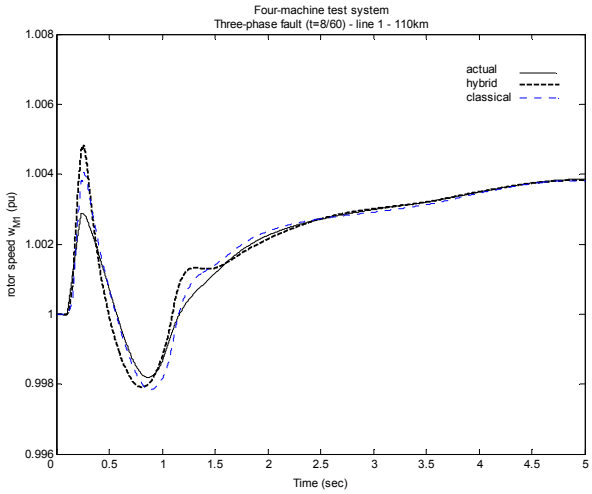

Fig. 10. Actual and estimated speed of generator M1 - three-phase fault at line 1

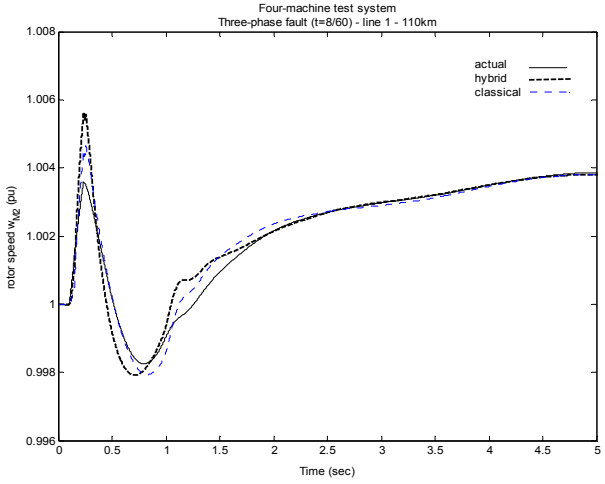

Fig. 11. Actual and estimated speed of generator M2 - three-phase fault at line 1

VI. CONCLUSION

This paper presented a novel approach to speed estimation of synchronous generator. The proposed estimator has hybrid architecture, combining a classical mathematical-based model of synchronous machine with a multi-layer feedforward artificial neural network. The paper has considered the design and performance analysis of the hybrid speed estimator. The performance was evaluated by incorporating the estimator in generator closed-loop governor system and simulating a wide range of operating conditions, including different disturbances, deviation of machine parameters, different types of synchronous generators, and various power system topologies. Results provided by the hybrid estimator were compared to those obtained using the classical mathematical-based estimator only and the AI-based estimator, respectively.

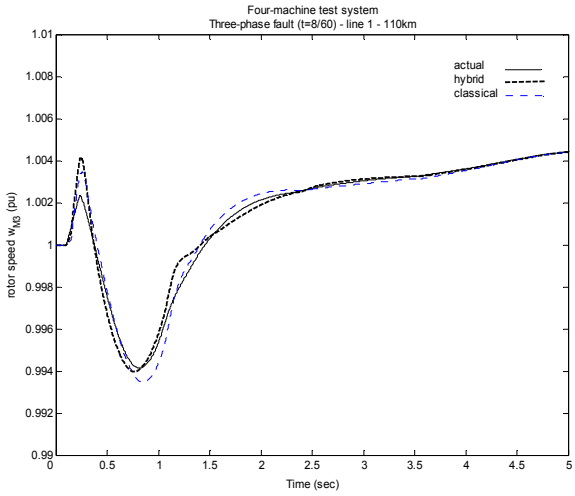

Fig. 12. Actual and estimated speed of generator M3 - three-phase fault at line 1

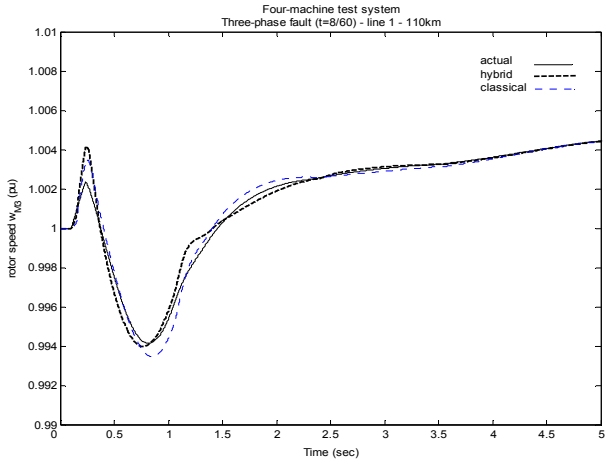

Fig. 13. Actual and estimated speed of generator M4 - three-phase fault at line 1

From the studies carried out it is concluded that the proposed approach is able to provide accurate estimates of generator rotor speed in a wide range of operating conditions, different from those used to train the ANN component. The hybrid estimator is stable, robust to deviations in machine parameters and noise. It outperforms the approach based on the use of artificial neural network only. While the hybrid estimator provided satisfactory response over the entire test range, the AI-based estimator failed outside the region implied by the training data.

Furthermore, the test results showed that the hybrid estimator is able to improve the performance of the classical mathematical-based model. In many tests, the hybrid estimator exhibit significant decrease in the amplitude and

phase estimation errors. A significant advantage of the hybrid approach lies in its independence on knowledge of any machine parameters. It should also be noted that the hybrid estimator is easily adaptable to new operating conditions by adding new representative examples in the training data base of the ANN component.

Finally, the simulation study confirmed that the proposed hybrid approach has potential to improve the performance of generator speed estimation in dynamic security assessment and control of power systems.

VII. APPENDIX

APPENDIX I

Parameters of the two 13.8 kV, 60 Hz synchronous generators in the power system model used for data base generation:

Pole pairs: p = 32
Inertia constant (pu-s): H = 3.7
Reactances (pu): $X_d = 1.305$; $X'_d = 0.296$; $X''_d = 0.252$; $X_q = 0.474$; $X''_q = 0.243$; $X_l = 0.18$
Time constants (s): $T'_d = 1.01$; $T''_d = 0.053$; $T''_{qo} = 0.1$
Stator resistance (pu): $R_s = 2.8544 \times 10^{-3}$

APPENDIX II

Parameters of the four 20 kV/900 MVA, 60 Hz round rotor generators of the power system model used in performance analysis:

Pole pairs: p = 4
Inertia constant (pu-s): H = 4.5 (Area 1), H = 6.175 (Area 2)
Reactances (pu): $X_d = 1.8$; $X'_d = 0.3$; $X''_d = 0.25$; $X_q = 1.7$; $X'_q = 0.55$; $X''_q = 0.25$; $X_l = 0.2$
Time constants (s): $T'_{d0} = 8$; $T''_{d0} = 0.03$; $T'_{q0} = 0.4$; $T''_{qo} = 0.05$
Stator resistance (pu): $R_s = 2.5 \times 10^{-3}$

VIII. REFERENCES

[1] P. Vas, *Sensorless vector and direct torque control*, Oxford University Press, Oxford, 1998

[2] P. Vas, *Artificial-intelligence-based electrical machines and drives. Application of fuzzy, neural, fuzzy-neural, and genetic-algorithm-based techniques*, Oxford University Press, New York, 1999

[3] A.F. Stronach, P. Vas, "Design, DSP implementation, and performance of artificial-intelligence-based speed estimators for electromechanical drives", *IEEE Proceedings on Control Theory Applications*, vol.145, no.2, March 1998, pp.197-203

[4] B. Kosko, *Neural networks and fuzzy systems – A dynamical systems approach to machine intelligence*, Pretince Hall, New Jersey, 1992

[5] K. Warwick, G.W. Irwin, K.J. Hunt (Eds.), *Neural networks for control and systems*, Oeter Perigrinus, 1992

[6] D. Fodor, F. Ionescu, D. Floricau, J.P. Six, P. Delarue, D. Diana, G. Griva, "Neural networks applied for induction motor speed sensorless estimation", *Proceedings of the IEEE International Symposium on Industrial Electronics*, ISIE '95, vol.1, 1995, page(s): 181–186

[7] S.H. Kim, T.S. Park, J.Y. Yoo, G.T. Park, "Speed-sensorless vector control of an induction motor using neural network speed estimation", *IEEE Transactions on Industrial Electronics*, vol.48, no.3, June 2001, pp. 609-614

[8] A. Del Angel, M. Glavic, L. Wehenkel, "Using Artificial Neural Networks to Estimate Rotor Angles and Speeds from Phasor Measurements", presented at *ISAP-2003*, Lemnos, Greece, September 2003

[9] J. Ghouili, A. Cheriti, "Comparison of the speed estimation by an adaptive observer and by a dynamic neural network observer for an asynchronous machine", *2000 Canadian Conference on Electrical and Computer Engineering*, vol.2, March 2000, pp. 1197 -1201

[10] Shao Zongkai,Ying Li, "The research for speed estimation of induction motor based on neural network", *Proceedings PIEMC 2000 The Third International Power Electronics and Motion Control Conference*, vol.3, pp. 1219 -1223

[11] Y. Oussar, G. Dreyfus, "How to be a Gray Box: Dynamic Semi-physical Modeling", *Neural Networks*, *invited paper,* vol. 14, pp. 1161-1172, 2001

[12] J.D. Glover, M. Sarma, *Power system analysis and design*, second edition, PWS Publishing Company, Boston, 1994

[13] D.R. Hush, B.G. Home, "Progress in supervised neural networks", *IEEE Signal Processing Magazine*, vol.10, Issue 1 , Jan.1993, pp. 8 -39

[14] M.T. Hagan, H.B. Demuth, M. Beale, *Neural network design*, PWS Publishing Company, 1996

[15] I. Kamwa, S. Martin, R. Grondin, "Comparison of artificial neural networks for on-line identification of a non-linear multivariable electromechanical process", *IEEE Instrumentation and Measurement Technology Conference*, Ottawa, Canada, 1997, pp.1106-1111

[16] K.H. Hornik, M. Stichcombe, H. White, "Multilayer feedforward networks are universal approximators", *Neural Networks*, vol2., no.5, 1989, pp. 359-366

[17] G. Sybille, P. Giroux, "Simulation of FACTS controllers using the MATLAB Power System Blockset and Hypersim real-time simulator", *IEEE Power Engineering Society Winter Meeting*, vol.1 , Jan. 2002, pp. 488-491

[18] H. Demuth, M. Beale, *Matlab Neural Network Toolbox User's Guide*, The MathWorks, Inc., Natick, MA, 2001

[19] A. Flexer, "Statistical evaluation of neural network experiments: minimum requirements and current practice", *Proceedings of the 13th European Meeting on Cybernetics and Systems Research, Austrian Society for Cybernetic Studies*, Vienna, p. 1005-1008, 1996

[20] S. Pillutla, S.M. Keyhani, I. Kamwa, "Neural Network Observers for On-line Tracking of Synchronous Generator parameters", *IEEE Transactions on Energy Conversion*, vol.14, no.1, 1999, pp. 23-30

[21] M. Klein, G.J. Rogers, S. Moorty, P. Kundur, "Analytical investigation of factors influencing PSS performance", *IEEE Transactions on Energy Conversion*, vol.7, no.3, 1992, pp. 382-390

[22] P. Kundur, Power system stability and control, McGraw-Hill, 1994